Computational Investigation of Antimicrobial Properties of Chitosan Based Zinc Oxide Nanocomposites

Abdulwahhab H. Majeed[1], Leqaa A. Mohammed[1], Israa K. Mohammed[1], Omar G. Hammoodi[1], Ali Shamil Abid Khan[1], Mustafa A. Ibrahim[1], Mustafa A. Alheety[2], Tarunpreet Singh[3], Ali Destegül[4] and Shankar Sehgal[5]

[1]*Department of Chemistry, College of Science, University of Diyala, 32001 Baqubah, Iraq*
[2]*Department of Nursing, Al-Hadi University College, 10053 Baghdad, Iraq*
[3]*Division of Research and Development, Lovely Professional University, 144401 Phagwara, India*
[4]*Department of Chemistry, Gaziosmanpaşa University, 60250 Tokat, Türkiye*
[5]*Department of Mechanical Engineering, University Institute of Engineering and Technology (UIET), Panjab University, 160014 Chandigarh, India*
abdulwahhab@uodiyala.edu.iq, liqaaadnan@uodiyala.edu.iq, israak@uodiyala.edu.iq, omerkazi@uodiyala.edu.iq, ali200shaml@gmail.com, mustafa.alialjburi@gmail.com, mustafa1990alheety@gmail.com, tarunpreet0512@gmail.com, melfoxx@gmail.com, sehgals@pu.ac.in

Keywords: Chitosan, ZnO NPs, Antimicrobial Evaluation, Schiff Base, Nanocomposites.

Abstract: The limited antimicrobial efficiency and stability of pure chitosan restrict its biomedical applications; therefore, in this study, chitosan was chemically modified via Schiff base formation and further combined with ZnO nanoparticles to enhance its structural and functional properties. Commercial chitosan was reacted with different aromatic aldehydes (p-N,N-dimethylaminobenzaldehyde, p-hydroxybenzaldehyde, and salicylaldehyde) to produce novel Schiff base derivatives (chitosan–p-N,N-dimethylaminobenzaldehyde, chitosan–p-hydroxybenzaldehyde, and chitosan–salicylaldehyde), whose structures were confirmed using FTIR spectroscopy. ZnO nanoparticles were synthesized and characterized using FTIR, XRD, EDX, and FE-SEM, revealing high-quality rod-shaped particles with diameters ranging from 39 to 63 nm. These nanoparticles were homogeneously incorporated into the chitosan Schiff base derivatives through stirring and ultrasonication, forming well-dispersed nanocomposites. The antimicrobial activity of both the pure Schiff base derivatives and the ZnO-containing nanocomposites was evaluated against Staphylococcus aureus, Staphylococcus epidermidis, Escherichia coli, Klebsiella sp., and Candida albicans, with all compounds exhibiting broad-spectrum activity and inhibition zones exceeding 40 mm. The high efficacy observed experimentally is consistent with theoretical mechanistic insights, where the synergistic effects of chitosan's cationic nature, Schiff base C=N interactions, hydrogen bonding, and ZnO-mediated ROS generation and Zn^{2+} release collectively contribute to membrane disruption, enzyme interference, and oxidative stress in microbial cells. Overall, this experimental and theoretical investigation confirms that the chitosan–aromatic Schiff base/ZnO nanocomposites are highly effective broad-spectrum antimicrobial agents with enhanced mechanistic functionality, supporting their potential application in biomedical fields.

1 INTRODUCTION

Chitin is a naturally occurring polymer, the N-deacetylated form of chitin is chitosan. Chitosan is one of the most abundant natural polymers owing to its significance in many applications. Chitin is also one of the most plentiful biopolymers and considered the second most abundant polymer after cellulose. Chitin and chitosan are present in the exoskeleton of insects and crustaceans and also in algae, fungi and yeasts. Chitosan is made up of glucosamine and N-acetylglucosamine units linked by β-(1→4) glycosidic bonds. These natural biopolymers display numerous unique biological activities, including antimicrobial, antitumor, and hemostatic activity, and enhance fast wound healing. This natural polymer has come under some consideration for biomedical applications due to its reported unique properties, including drug and gene delivery systems, and tissue engineering and wound healing [1]. Chitosan poly

saccharides antimicrobial activity is dependent on many structural factors, such as molecular weight and degree of deacetylation, and some environmental factors such as pH, and presence of ions such as Ca^{2+} and Mg^{2+} [2]. These include the presence of the amino groups of glucosamine in glucosamine units and are responsible for the antimicrobial properties. It is noteworthy that, to the low pH, the efficacy of these antimicrobial properties is further increased. At acidic pH, the activity enhancement is attributed to the protonation of the amino groups, which increases their affinity to the cell membrane of microorganisms and subsequently leads to more effective membrane disruption and inhibition of microbial growth. Antibacterial activities of the chitosan were reported as variable [3], which is likely due both to properties of the chitosan used and assay conditions so that results may be less comparable across studies [3].

Due to the rigid hydrogen bonding and crystalline structures of chitosan, it is generally insoluble in organic solvents and in neutral or alkaline media, but it can dissolve in dilute acids. Chitosan contains both amino and hydroxyl groups, both of which are essential for subsequent chemical modifications that can improve and broaden chitosans applicability [4]. In particular, its amino groups can undergo a reaction with aldehydes and ketones to generate Schiff bases which have been synthesized and characterized for their improved physicochemical and biological properties. Depending on the nature of the substituent, heterosubstituted Schiff bases have also shown a broad spectrum of activities such as antiviral, antifungal, antioxidant, antiinflammatory, antitumor, anticancer, antibacterial and antipyretic effects [2]. Avoiding paraphrasing a sentence too closely. Aided by a moiety derived from natural products, such as Schiff bases, chitosan composite matrixes have also improved their activity to bind with metal ions, leading to increased biological activity and potential heterogeneous catalysts [5]. Our working hypothesis is that the dual strategies of Schiff base functionalization and incorporation of ZnO nanoparticles will work synergistically to increase the antimicrobial activity of the nanofibrous scaffolds by enhancing surface charge interactions and inducing the generation of reactive oxygen species. During the evolution of chitosan-based natural polymer Schiff base derivatives or adducts Schiff base semisynthetic derivatives, nanomaterials are important on the biological activity of these chitosan materials especially against microbial activities including bacteria and fungi [6]-[9]. Chitins chitosans is a very promising material for medical applications due to its non-toxicity, biodegradability and biocompatibility. The biological and physical properties of chitosan are improved after chemical modification and the formation of Schiff base compounds. The coordination of Schiff bases to metals enhances their biological activity [10]. A large increase in antimicrobial activity is achieved when Schiff-chitosan bases are combined with the use of nanomaterials (ZnO,Ag,TiO_2,CuO, Fe_2O_3, … etc.). Antibacterial; Nanomaterials; Chitosan; Composite-material impregnation;Novel preparation Inherited from their small sizeNand their volume-to-surface area ratios, nanoparticles grant to higher interaction with biological targets making Schiffs–chitosan bases effects on microbes more potent. Moreover, these nanocomposites can also be prepared and used for more efficient drug delivery that can selectively target to the site of infections more efficiently and with less side effects. The nanomaterials in this study also facilitate the permeation of the antibacterial and antifungal compounds across bacterial and fungal cell membranes, thereby disrupting critical activities within cellular by inhibiting growth of the microbes. It can provide higher antimicrobial activity and overcome microbial resistance against conventional treatment, by improving biological efficacy and promoting microbial cell interaction, thus opening new perspectives in medical therapy [11].

The objective of this study is to prepare chitosan-Schiff bases from the reaction of chitosan with the aldehydes p-N,N-dimethylamino benzaldehyde, p-hydroxy benzaldehyde and salicyl aldehyde. Moreover, nano-zinc oxide nanoparticles were synthesized and were mixed with prepared Schiff base compounds to produce nano-polymer composites. In addition, the active biological activity of the synthesized compounds was tested against (Staphylococcus aurous, Staphylococcus epidermidis, Escherichia coli, Klebsiella sp. and Candida albicans).

2 EXPERIMENTAL

2.1 Chemicals

Chemicals and solvents obtained from various suppliers, such as Sigma-Aldrich, Riedel-de Haën, or SDH, were used this study. All materials were used as received, without any further purification.

2.2 Devices

Multiple techniques were employed to characterize the synthesized compounds, including FTIR, XRD,

EDX, and FE-SEM. An infrared spectrometer, a Perkin Elmer FTIR-65, was used for FTIR analysis. Additionally, an X-ray detector (Philips/PW1730, Cu, Kα = 1.5406 Å) was used to analyze the composition of the material. The surface morphology of the materials was examined using a TESCAN MAIA3 scanning electron microscope (FE-SEM).

2.3 Procedures

2.3.1 Preparation of Chitosan Solution

At room temperature, 1 g of chitosan was dissolved in 50 mL of a 2% (v/v) acetic acid solution under continuous stirring. After 6 hour of constant stirring, this mixture produced a translucent, colorless chitosan solution.

2.3.2 Preparation of Chitosan- Schiff Base Derivatives

Chitosan, 0.5 g, was dissolved in 50 mL of a 2% acetic acid solution at room temperature. The resulting solution was continuously stirred for 6 hours, resulting in a colorless chitosan solution. Next, 0.25 g of each aldehyde (p-N,N-dimethylamino benzaldehyde, p-hydroxy benzaldehyde and salicylaldehyde) was dissolved in 50 mL of ethanol. The aldehyde solution was added dropwise to the chitosan solution while maintaining stirring at 50 °C. After the addition was complete, the reaction mixture was stirred for another 6 hours at 50°C. The resulting gelatinous product was washed several times with ethanol to remove unreacted aldehyde, followed by washing with 3% sodium hydroxide to remove residual acetic acid. Afterwards, the substance was rinsed 3 times with deionized water to eliminate any excess NaOH. Ultimately, as illustrated in Figure 1, it was dried at 80 °C for 6 hours [12].

2.3.3 Preparation of Zinc Oxide Nanoparticles (ZnO NPs)

The synthesis of ZnO nanoparticles (ZnO NPs) was carried out through the following steps: Initially, 2.195 g of zinc acetate dihydrate ($Zn(CH_3COO)_2{\cdot}2H_2O$) was completely dissolved in 100 mL of deionized water to form solution A. Concurrently, 0.8 g of sodium hydroxide (NaOH) was dissolved in 50 mL of deionized water to form solution B. Solution A was then gradually added to solution B dropwise, while maintaining the temperature at 60–65°C under vigorous stirring for 1 hour. The resulting mixture was allowed to age for 3 hours under the same temperature and stirring conditions. Following this, the the formed white precipitate was cooled to room temperature, filtered, and rinsed several times with deionized water to ensure purity. Finally, the precipitate was dried in an oven at 80°C for 8 hours, yielding the desired ZnO nanoparticles [13].

2.3.4 Synthesis of Chitosan-Schiff base/ ZnO Nanocomposites

A mixture of chitosan–Schiff base derivatives 1.8 g including chitosan–p-N,N-dimethylamino benz-aldehyde, chitosan–p-hydroxybenzaldehyde, and chitosan salicylaldehyde was dissolved in 20 mL of 2% (v/v) acetic acid and stirred at 70°C for 1 hour. Then, add 0.3 g of zinc oxide to each solution and let it stir for 30 minutes. After that, transfer the mixture to an ultrasonic device and allow it to homogenize for 2 hours until the process is complete.

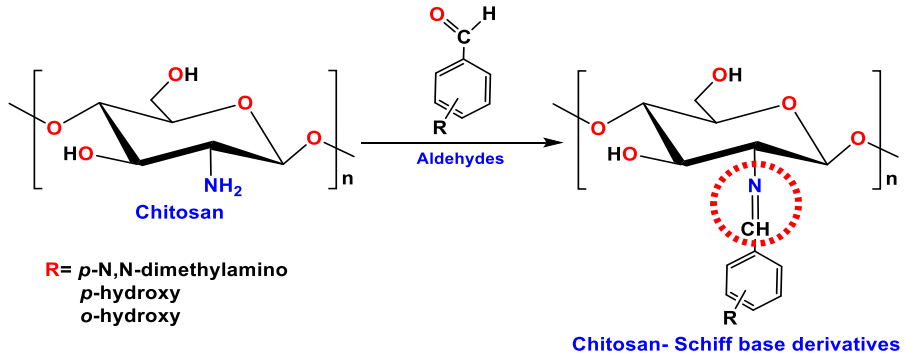

Figure 1: The chemical reaction for the preparation of Chitosan Schiff bases using [(p-N,N-dimethylamino benzaldehyde), (p-hydroxy benzaldehyde), and (salicylaldehyde)].

3 RESULT AND DISCUSSION

3.1 Characterization of ZnO NPs:

3.1.1 FTIR of ZnO NPs

Figure 2 displays the FTIR spectrum of zinc oxide nanoparticles prepared by the mentioned chemical method. The spectrum exhibits a broad absorption band at 3379 cm^{-1}, which corresponds to the O–H stretching vibrations of surface-adsorbed water molecules on the ZnO nanoparticles. A band centered at 1567 cm^{-1} is also observed, corresponding the bending vibration of the OH group of the same water molecules. The stretching vibration of the Zn-O bond in ZnO NPs is responsible for the band that is centered in the 419 cm^{-1} regions [14].

3.1.2 XRD of ZnO NPs

XRD is a critical technique used to determine the structure of crystals, phase composition, and purity of materials as well as to determine the crystalline size of particles. It analyzes the diffraction pattern of X-rays diffracted by atomic levels within the crystal, providing detailed information about the internal structure of the materials [15] - [19]. The XRD pattern of ZnO nanoparticles (Fig. 3) shows several sharp diffraction peaks at 2θ values of (2θ = 31.7189, 34.3224, 36.2830, 47.6227, 54.1320, 56.5642, 59.9838, 62.9247, 66.4878, 68.0870, 69.1588, 72.7933, 77.1045˚) confirming the high crystallinity of ZnO. The obtained diffraction data are in good agreement with the standard JCPDS card No. 36-1451 and previously reported studies. As a result, the synthesized zinc oxide is considered to be of high purity, with no interference detected in the analyzed spectrum.

3.1.3 EDX of ZnO NPs

The produced zinc oxide nanoparticles' purity is verified by EDX analysis. The EDX spectrum of ZnO nanoparticles displays three characteristic peaks (Zn Lα, Zn Kα, and Zn Kβ) in the energy range of 1.01–9.60 keV, corresponding to zinc. An additional peak corresponding to oxygen centered at 0.50 keV, as shown in Figure 4. This analysis confirms the high purity of the manufactured zinc oxide nanoparticles, as no additional impurity signals were observed, and these results are very consistent with previously studies [20]-[22].

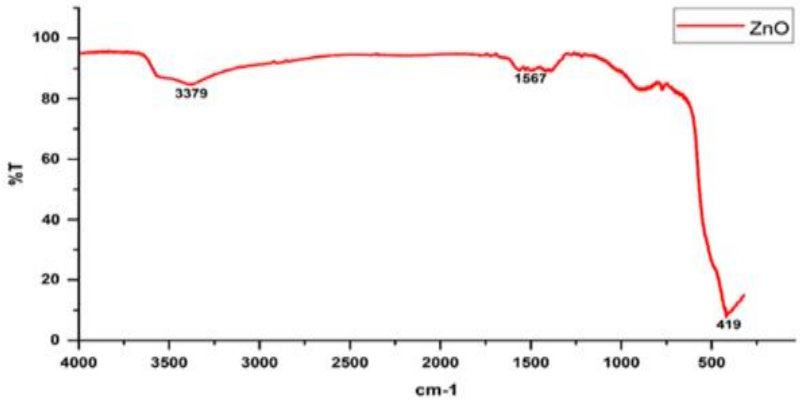

Figure 2: FTIR of ZnO nanoparticles.

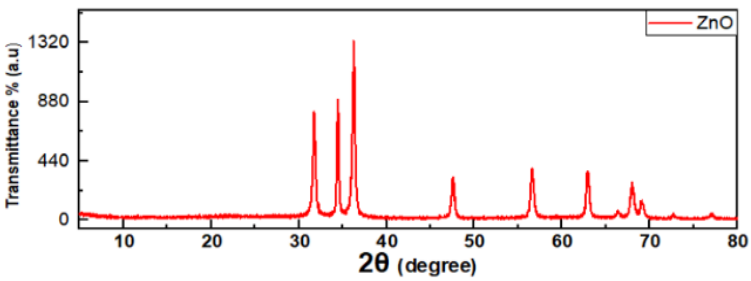

Figure 3: XRD of ZnO nanoparticles.

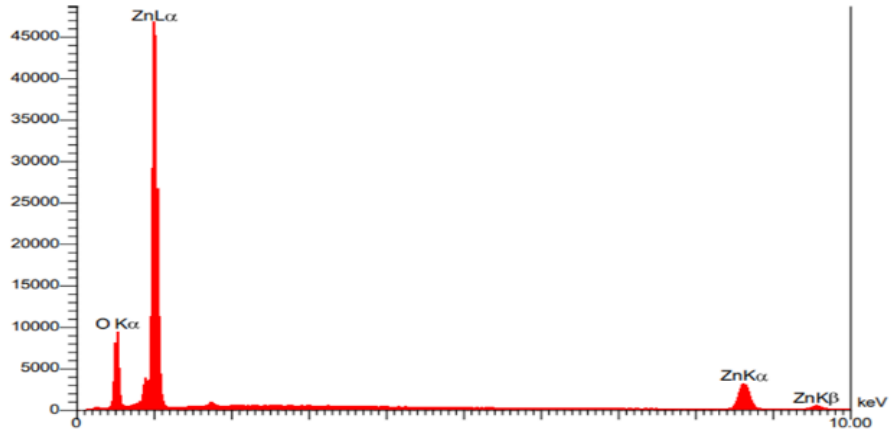

Figure 4: EDX of ZnO nanoparticles.

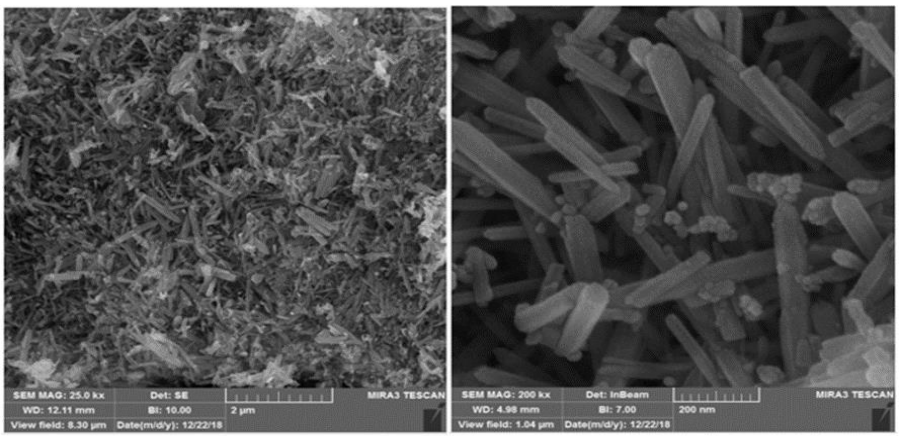

Figure 5: FE-SEM of ZnO nanoparticles.

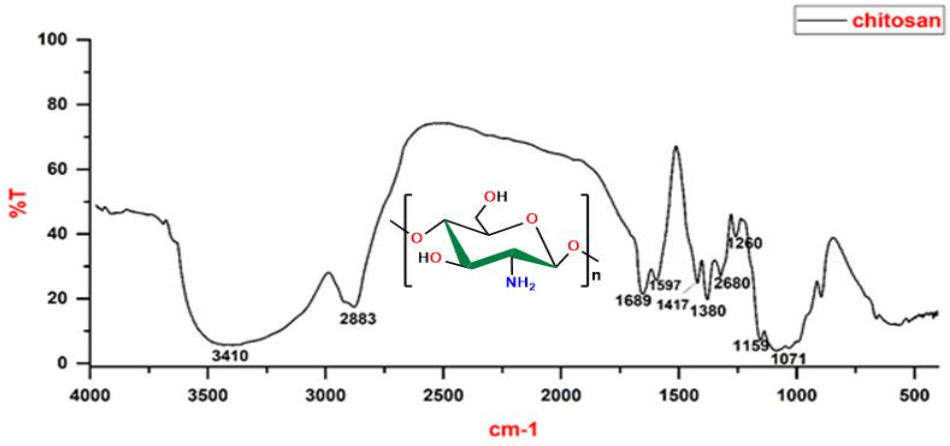

Figure 6: FTIR of pure chitosan.

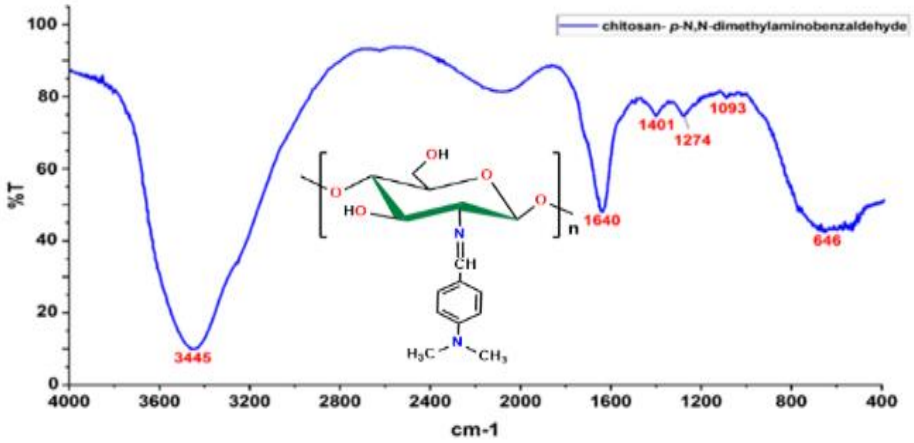

Figure 7: FTIR of chitosan- p-N,N-dimethyl amino benzaldehyde Schiff bases.

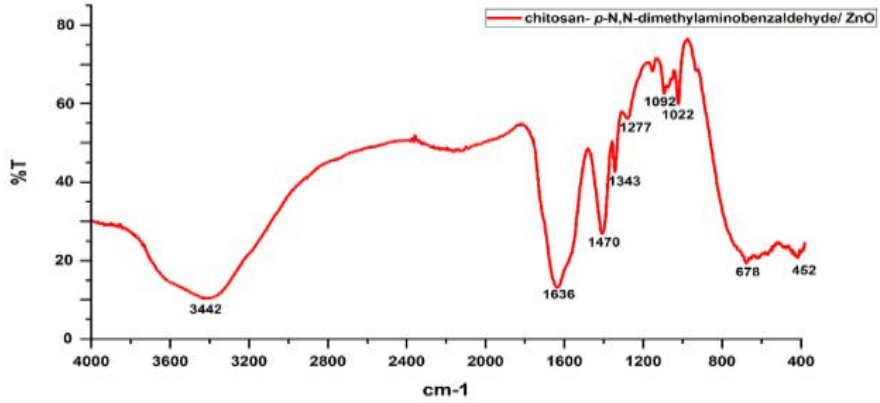

Figure 8: FTIR of chitosan- p-N,N-dimethyl amino benzaldehyde Schiff bases with ZnO NPs.

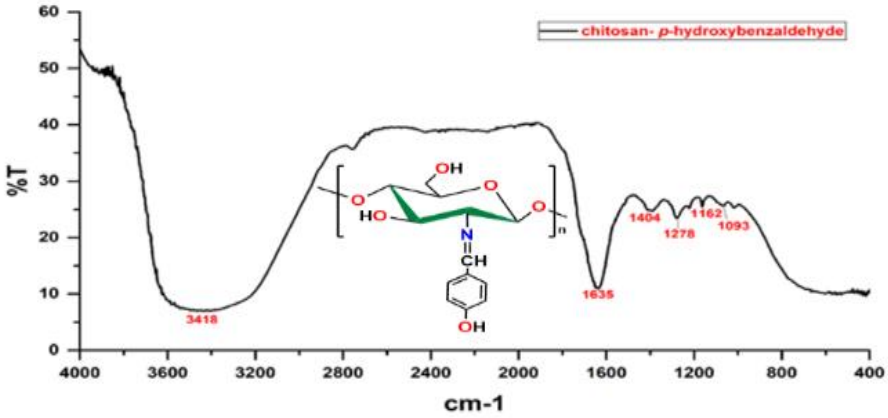

Figure 9: FTIR of chitosan- p-hydroxy benzaldehyde Schiff bases.

3.1.4 FE-SEM of ZnO NPs

FE-SEM analysis was used to determine the sizes and morphology of the produced ZnO NPs. The FE-SEM micrograph of ZnO nanoparticles (Fig. 5) reveals rod-like structures with varying lengths and diameters ranging from 39 to 63 nm.

3.2 Characterization of Chitosan Derivatives

3.2.1 FTIR of pure Chitosan

The functional groups included in chitosan and its produced derivatives are identified by analyzing their FTIR spectra. The pure chitosan's FTIR spectrum is shown in Figure 6. The strong and broad absorption band centered at 3410 cm^{-1} corresponds to the O–H stretching vibrations of the hydroxyl groups in chitosan molecules. The absorption band centered at 2883 cm^{-1} is attributed to the C–H stretching vibrations of the aliphatic groups. These bands are representative of polysaccharides and are also observed in the spectra of other polysaccharides such as xylan, glucans, and carrageenan's [23]-[25]. The presence of bands at 1689 and 1597 cm^{-1} can be attributed to bending vibration amine groups (-NH_2), It is also noted that the amine group is not present in the stretching region due to its merging with the hydroxyl group because it is located in the same region. The band at 1417 cm^{-1} confirms the existence of the -CH_2 bending vibration. The C-O stretching vibration is represented by the band at 1159 cm-1. Moreover, the intense band observed at 1071 cm^{-1} is ascribed to the stretching vibrations of β-(1→4) glycosidic bonds in polysaccharides, which are part of the C–O–C linkage in the chitosan backbone. These spectral features align with those reported for chitosan samples in previous research [26].

3.2.2 FTIR of Chitosan- p-N,N-dimethylamino benzaldehyde Schiff Bases

The FTIR spectrum of the chitosan-p-N,N-Dimethyl amino benzaldehyde Schiff bases is shown in Figure 7. There is a noticeable broad peak at 3418 cm^{-1}, which corresponds to the O-H groups' stretching vibrations. Moreover, the O-H groups of chitosan and the –NH_2 groups of the amine at the para position are shown to form intermolecular hydrogen bonds by this peak. Clear proof of the successful synthesis of the Schiff base is provided by the conspicuous band centered at 1640 cm^{-1}, which is due to the imine group (C=N). This group is generated by a reaction between the amino group of chitosan and the carbonyl group of the aldehyde. In addition, the band centered at 1401 cm^{-1} indicates the -CH_2 bending vibration, which also confirms the structural integrity of the chitosan-p-N,N-Dimethyl amino benzaldehyde Schiff bases. Moreover, the band centered at 1093 cm^{-1} is due to the stretching vibrations of the C-O-C group of polysaccharides [27].

3.2.3 FTIR of Chitosan-p-N,N-dimethyl aminobenzaldehyde Schiff Bases with ZnO NPs

The FTIR spectrum of chitosan-p-N,N-dimethyl aminobenzaldehyde schiff bases with ZnO NPs is presented in Figure 8. After adding nano-zinc oxide, some changes are observed in the FTIR peaks of the prepared compound, as a new peak belonging to zinc oxide appears, and a slight shift is observed in some of the peaks. In general, the FTIR spectrum illustrations a number of peaks centered at 3442, 1636, 1470, 1277, and 1092 cm^{-1}, which belong to -O-H, -C=N- (schiff base structures), -CH_2, C-O, and the stretching vibrations of the -C-O-C- of β (1-4) glycosidic bonds of polysaccharides, respectively. It is likewise noted that a band seems at 452 cm^{-1}, which belongs to Zn-O. The noticeable shift in the hydroxyl and imine peaks is evidence of the occurrence of a physical interaction between the prepared compound and nano-zinc oxide.

3.2.4 FTIR of Chitosan-p-hydroxy Benzaldehyde Schiff Bases

Figure 9 provides a comprehensive FTIR spectrum of the chitosan-p-hydroxy benzaldehyde Schiff base. An abroad peak at 3418 cm^{-1} agrees to the stretching vibrations of O-H groups and intermolecular hydrogen bonding. The strong band centered at 1635 cm^{-1} belongs to the imine group (C=N), formed from the reaction between the amine group of chitosan and the carbonyl group of the aldehyde, indicating successful Schiff base synthesis. This is evidence of the success of the reaction occurring between chitosan and aldehyde. The bending vibration of -CH_2 was established by the band positioned at 1417 cm^{-1}. The band placed at 1162 cm^{-1} correspond to the stretching vibration of C-O. Moreover, the band centered at 1093 cm^{-1} can be attributed to the stretching vibrations of C-O-C bridge of polysaccharides [28].

3.2.5 FTIR of Chitosan- p-hydroxy benzaldehyde Schiff bases with ZnONPs

Figure 10 represents the FTIR analysis of chitosan- p-hydroxy benzaldehyde schiff bases with ZnO NPs. It is noted from the figure that a number of peaks appear spread within the range 400 - 4000 cm^{-1}, which represent the real FTIR spectrum of the prepared

compound. The figure contains a number of peaks centered at 3437, 1638, 1409, 1164 and 1094 cm^{-1}, which belong to groups of -O-H, -C=N- (schiff bases), $-CH_2$, -C-O and the stretching vibrations of -C-O-C- bridge of polysaccharides, respectively. It is besides noted that a band looks at 423 cm^{-1}, which belongs to Zn-O, which represents the main group in zinc oxide. The shifting occurring in the hydroxyl and imine peaks is good evidence of the physical interaction between the prepared compound and nano-zinc oxide.

3.2.6 FTIR of Chitosan- Salicylaldehyde Schiff Bases

FTIR analysis was performed to identify the functional groups present in the prepared chitosan-salicylaldehyde Schiff bases presented in Figure 11. The strong and broad band at 3439 cm^{-1} is associated with the stretching vibrations of the OH groups, which expand as a result of hydrogen bonding interactions. The strong band positioned at 1638 cm^{-1} relates to the stretching vibration of imine (-C=N-) groups, confirming the formation of Schiff bases. The band at 1392 cm^{-1} indicates the bending vibration of the methylene $-CH_2$ group, while the band at 1275 cm-1 is associated to the stretching vibrations of C-O. Moreover, the observed band at 1096 cm^{-1} is due to the stretching vibrations of the C-O-C bridge in the polysaccharides. The characteristic band of $-NH_2$ groups in chitosan is noticeably diminished, indicating their participation in the reaction with the aromatic aldehyde (salicylaldehyde) to form the Schiff base compounds [29].

3.2.7 FTIR of Chitosan- Salicylaldehyde Schiff Bases with ZnO NPs

After adding nano zinc oxide to the chitosan-salicylaldehyde schiff bases compound, some changes are observed in the FTIR peaks of the new compound, as a new peak belonging to zinc oxide is observed, and a slight shift is observed in some of the peaks. Figure 12 displays the FTIR spectrum of chitosan-Salicylaldehyde Schiff bases with ZnO NPs. The spectrum shows the presence of peaks centered at 3444, 1633, 1407, 1343, and 1053 cm^{-1}, which belong to -O-H, C=N-, $-CH_2$, and the C-O-C linkage stretching vibrations of polysaccharides, respectively. The -OH peak appeared broad due to hydrogen bonding between the -OH group in salicylaldehyde and the -OH groups in chitosan. Additionally, a notable peak emerges at 421 cm^{-1}, indicative of the Zn-O bond. The noticeable shift in the hydroxyl and imine peaks is evidence of the occurrence of a physical interaction between the prepared compound and nano-zinc oxide.

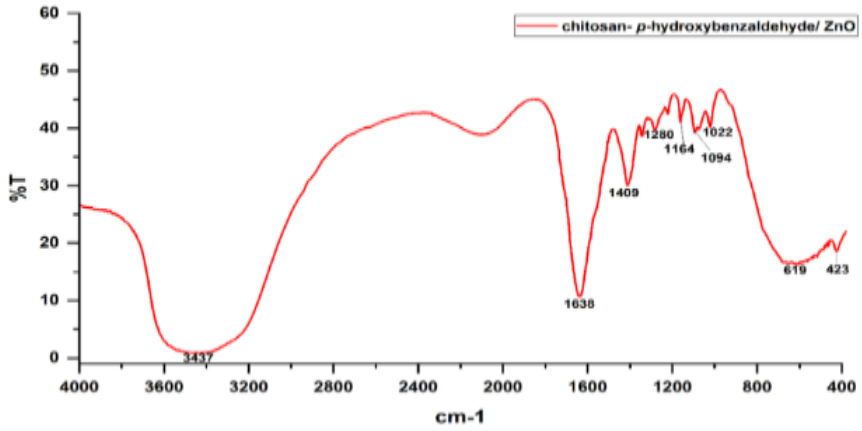

Figure 10: FTIR of chitosan- p-hydroxy benzaldehyde Schiff bases with ZnO NPs.

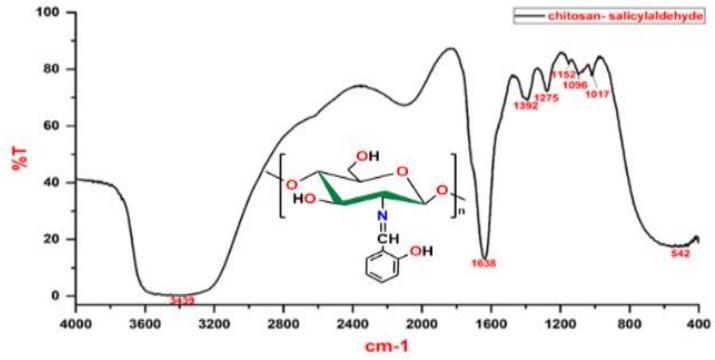

Figure 11: FTIR of chitosan- Salicyl aldehyde Schiff bases.

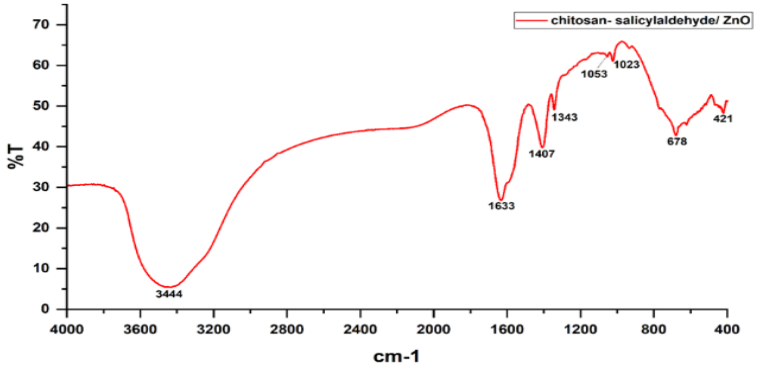

Figure 12: FTIR of chitosan- Salicylaldehyde Schiff bases with ZnO NPs.

3.3 The Biological Activity of Prepared Compounds

The compounds showed biological activity against a variety of microorganisms after synthesis and characterization. Two Gram-positive bacteria (Staphylococcus aureus and Staphylococcus epidermidis), and two Gram-negative bacteria (Escherichia coli and Klebsiella species) were examined for the evaluation. Moreover, the antifungal activity of the compounds was evaluated against Candida albicans. This study delineates a wideranging analysis towards evaluating the impact of synthesized compounds towards inhibiting the growth of selected number of bacterial and fungal pathogens which may send an indication to be potential antimicrobial agents. Synthesis Compounds The synthesized compounds were screened for the antibacterial activity at the concentration 30mg/mL of a substance dissolved in dimethyl sulfoxide (DMSO). Method agar well diffusion with Mueller–Hinton agar medium using McFarland turbidimetric method to the same standard concentration of bacteria. Tables 1 show the inhibition zones (in mm) generated from these interactions and Figures 13 and 14 show the resulting inhibition zones. This enabled a side-by-side comparison of efficacy of the compounds in inhibiting bacterial growth. Compounds were all estimated as high activity (inhibition zone => 40 mm) against all microorganisms (Staphylococcus aureus, Staphylococcus epidermidis, Escherichia coli, Klebsiella sp, and Candida albicans). This proves their superiority in action towards these pathogens, and indicates their potential use so long as their toxicity does not harm human health or the environment [30].

Table 1: The inhibition zones of prepared compounds.

Comp.	The Inhibition Zones of Microbes (mm)				
	S. aureus	S. epidermidis	E. coli	K. pneumonia	C. albicans
A1	> 40	> 40	> 40	> 40	> 40
A2	> 40	> 40	> 40	> 40	> 40
A3	> 40	> 40	> 40	> 40	> 40
B4	> 40	> 40	> 40	> 40	> 40
B5	> 40	> 40	> 40	> 40	> 40
B6	> 40	> 40	> 40	> 40	> 40
PG	0	0	0	0	---
FLU	---	---	---	---	0

Where:

- A1: chitosan- p-N,N- dimethyl amino benzaldehyde.
- A2: Chitosan- p-hydroxy benzaldehyde.
- A3: Chitosan- Salicylaldehyde.
- B4: Chitosan- Salicylaldehyde/ ZnO NPs.
- B5: Chitosan- p-N,N- dimethyl amino benzaldehyde/ ZnO NPs.
- B6: Chitosan- p-hydroxy benzaldehyde/ ZnO NPs.
- PG: Penicillin.
- FLU: Fluconazole.

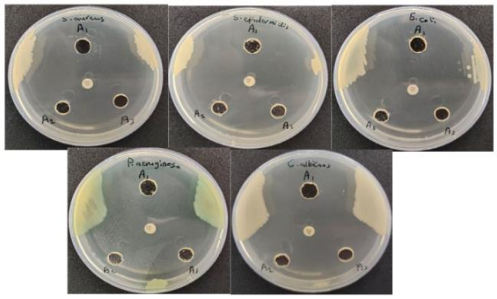

Figure 13: Effects of the chitosan-aldehyde schiff bases (A1, A2 and A3) against the microorganisms.

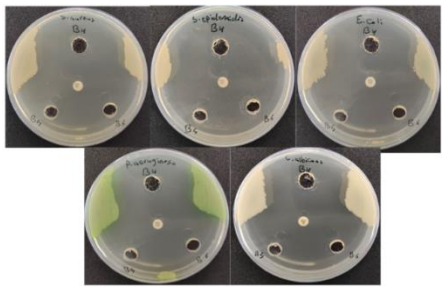

Figure 14: Effects of the chitosan-aldehyde schiff bases/ ZnO NPs (B4, B5 and B6) against the microorganisms.

3.4 Theoretical Interpretation of Antimicrobial Activity of Chitosan–Schiff Base Compounds

This theoretical study provides an interpretation of the high antimicrobial activity observed for chitosan–Schiff base derivatives (A1–A3) and their ZnO nanoparticle-loaded hybrid counterparts (B4–B6). All compounds demonstrated inhibition zones greater than 40 mm against Gram-positive bacteria (Staphylococcus aureus, Staphylococcus epidermidis), Gram-negative bacteria (Escherichia coli, Klebsiella pneumoniae), and the fungal strain Candida albicans. Chitosan contributes strong cationic interactions with negatively charged microbial membranes, increasing membrane permeability and leading to leakage of intracellular contents. The Schiff base (C=N) linkage enhances electronic interactions and promotes hydrogen bonding with cell wall proteins. Functional substituents influence reactivity: N,N-dimethylamino groups increase basicity and electrostatic attraction, while hydroxyl groups enhance hydrogen bonding and potential chelation. ZnO-loaded hybrids (B4–B6) provide additional mechanisms, including release of Zn^{2+} ions that bind to thiol-containing proteins, and generation of reactive oxygen species (ROS), leading to oxidative stress, membrane disruption, and DNA damage (Table 2). These combined effects justify the exceptionally high antimicrobial activity observed experimentally.

Figure 15 represents the antimicrobial activity of all synthesized compounds (A1–A3 and B4–B6). All compounds exhibited inhibition zones greater than 40 mm, indicating strong broad-spectrum activity against all tested microorganisms (Gram-positive, Gram-negative bacteria, and Candida). It is evident that both the organic Schiff-base–chitosan derivatives and the ZnO-loaded hybrids have very high efficacy, far exceeding the control antibiotics Penicillin and Fluconazole (0 mm). This confirms that the compounds act through broad-spectrum mechanisms, likely due to the cationic nature of chitosan and Schiff base interactions.

While Figure 16 compares the activity of the organic compounds alone (A1–A3) versus their ZnO-hybrid counterparts (B4–B6). All inhibition zones are approximately equal (~40 mm), indicating that the addition of ZnO did not significantly increase the inhibition diameter in the agar well diffusion test. Theoretically, ZnO provides additional mechanisms such as reactive oxygen species (ROS) generation, Zn^{2+} ion release, and enhanced membrane interactions. However, in this experiment, all compounds reached the maximum inhibition limit, so the effect of ZnO is not visually apparent.

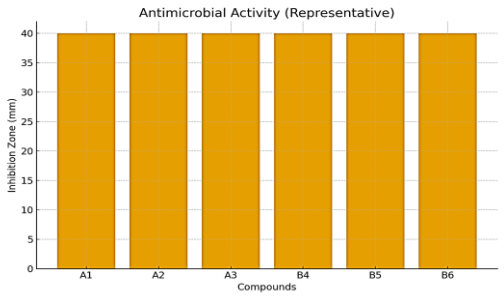

Figure 15: Antimicrobial activity (representative bar chart).

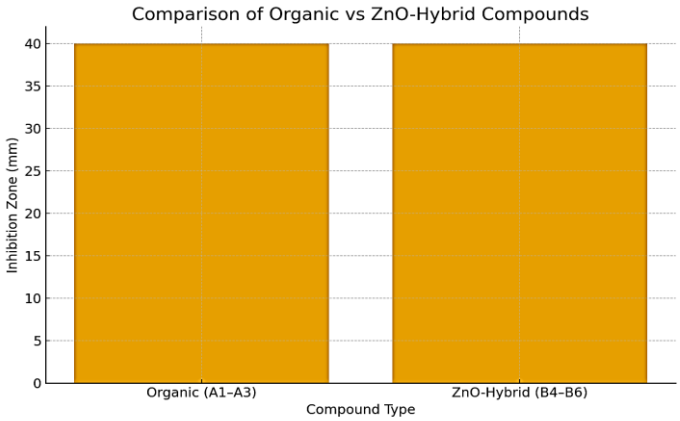

Figure 16: Comparison between organic and ZnO-hybrid compounds.

Table 2: Theoretical properties, mechanistic explanation, and expected antimicrobial activity of chitosan-schiff Base / ZnO nanocomposites.

Comp.	Functional Group	Theoretical Properties	Mechanistic Explanation	Expected Activity
A1	p-N,N-dimethylamino	High basicity; strong charge	Electrostatic membrane disruption	Very high
A2	p-hydroxy	High H-bonding ability	Protein binding; membrane disruption	Very high
A3	Salicylaldehyde	Chelation ability	Enzyme interaction; membrane effects	Very high
B4	A3 + ZnO	ROS + Zn^{2+} release	Dual oxidative and membrane attack	Higher
B5	A1 + ZnO	Strong charge + ROS	Electrostatic + oxidative stress	Higher
B6	A2 + ZnO	H-bonding + ROS	Membrane penetration + oxidation	Higher

4 CONCLUSIONS

The prepared chitosan–aldehyde derivatives and their chitosan–aldehyde/ZnO nanocomposites were characterized using FT-IR, XRD, EDX, and FE-SEM to confirm chemical structure, composition, and morphology. FT-IR spectra of Schiff base derivatives (chitosan–p-N,N-dimethyl amino benzaldehyde, chitosan–p-hydroxy benzaldehyde, and chitosan–salicylaldehyde) showed C=N stretching vibrations, indicating successful formation, while the ZnO-containing nanocomposites displayed additional Zn–O bands, confirming nanoparticle incorporation. XRD revealed the crystalline hexagonal wurtzite structure of ZnO, and EDX confirmed uniform zinc distribution. FE-SEM showed nanorod-like ZnO particles with diameters of 39–63 nm homogeneously dispersed in the chitosan matrix. Experimentally, all compounds exhibited broad-spectrum antimicrobial activity (>40 mm inhibition zones) against Gram-positive, Gram-negative bacteria, and Candida albicans, as summarized in the table. Theoretically, the high activity is attributed to synergistic effects of chitosan's cationic nature, Schiff base C=N interactions, hydrogen bonding, and ZnO-mediated mechanisms, including ROS generation and Zn^{2+} release, leading to membrane disruption, enzyme interference, and oxidative stress. While all compounds reached maximum inhibition experimentally, ZnO hybrids provide additional mechanistic advantages under varying conditions. Overall, combining experimental and theoretical insights demonstrates that these chitosan–aromatic Schiff base/ZnO nanocomposites are a promising platform for broad-spectrum antimicrobial applications.

REFERENCES

[1] T. M. Tamer et al., "Synthesis, characterization and antimicrobial evaluation of two aromatic chitosan Schiff base derivatives," Process Biochemistry, vol. 51, no. 10, pp. 1721-1730, Oct. 2016.

[2] C. YC Su, "Relationship between antibacterial activity of chitosan and surface characteristics of cell wall," Acta Pharmacologica Sinica, vol. 25, no. 7, 2024.

[3] U. K. Biswas, A. Bose, B. Ghosh, and S. Sharma, "An insight into chemically modified chitosan and their biological, pharmaceutical, and medical applications: A review," International Journal of Biological Macromolecules, vol. 303, p. 140612, Feb. 2025.

[4] M. A. Alheety et al., "A review on benzimidazole heterocyclic compounds: Synthesis and their medicinal activity applications," SynOpen, vol. 7, no. 4, pp. 652-673, Aug. 2023.

[5] F. Fadil, N. D. N. Affandi, M. I. Misnon, N. N. Bonnia, A. M. Harun, and M. K. Alam, "Review on electrospun nanofiber-applied products," Polymers, vol. 13, no. 13, p. 2087, Jun. 2021.

[6] A. A. Jarullah, W. B. Ali, and O. W. Mohammed, "Synthesis and antibacterial evaluation of ligand 3-(2-amino-5-b-benzoyl-phenylimino)-1,3-dihydro-indol-2-one and its complexes with ions of Co(II), Ni(II), Cu(II), and Zn(II)," AIP Conference Proceedings, vol. 2516, pp. 040012-040012, Jan. 2023.

[7] A. A. Jarullah, N. M. Khamees, and A.-D. Musa, "Synthesis of ZnO nanoparticle and utilized as a drug carrier to treat leukemia," Indonesian Journal of Chemistry, vol. 23, no. 4, pp. 1071-1071, Aug. 2023.

[8] A. A. Jarullah, M. Hammadi, and K. H. Hassan, "Green synthesis of nano Zn3(PO4)2 using Curcuma extract and their effect on SK-OV-3 human ovarian cancer cell lines: Effects of nano Zn3(PO4)2 at human ovarian cancer cell," Biological Sciences - PJSIR, vol. 68, no. 2, pp. 166-171, 2025, [Accessed: Oct. 25, 2025].

[9] M. A. Alheety, A. A. Jarullah, M. Y. Mohammed, A. R. Mahmood, and A. Aydin, "Pt phosphor-, oxygen-rich complexes: One pot synthesis, characterization, molecular docking and antiproliferative study," Inorganica Chimica Acta, vol. 548, p. 121395, Jan. 2023.

[10] M. M. Gaafar, F. M. Eltaweel, H. A. Fouda, and M. Y. Abdelaal, "Synthesis of novel chitosan Schiff base and its ZnO nanocomposite for removal of synthetic dye, antimicrobial, and cytotoxicity activity," Journal of Bioactive and Compatible Polymers, vol. 37, no. 5, pp. 359-380, Sep. 2022.

[11] R. A. Alharbi, F. M. Alminderej, N. F. Al-Harby, N. Y. Elmehbad, and N. A. Mohamed, "Design, synthesis, and characterization of novel bis-uracil chitosan hydrogels modified with zinc oxide nanoparticles for boosting their antimicrobial activity," Polymers, vol. 15, no. 4, p. 980, Feb. 2023.

[12] L. El Hamdaoui, M. El Marouani, M. El Bouchti, F. Kifani-Sahban, and M. El Moussaouiti, "Thermal stability, kinetic degradation and lifetime prediction of chitosan Schiff bases derived from aromatic aldehydes," ChemistrySelect, vol. 6, no. 3, pp. 306-317, Jan. 2021.

[13] N. F. Alheety et al., "Antiproliferative and antimicrobial studies of novel organic-inorganic nanohybrids of ethyl 2-((5-methoxy-1H-benzo[d]imidazol-2-yl)thio)acetate (EMBIA) with TiO2 and ZnO," Journal of Molecular Structure, vol. 1274, pp. 134489-134489, Feb. 2023.

[14] M. Nouri-Mashiran, L. Taghavi, E. Fataei, G. Ebrahimzadeh-Rajaei, and M. Ramezani, "Green synthesis of ZnO nanoparticles and comparison of 2,4-dinitrophenol removal efficiency using photocatalytic, sonocatalytic, and adsorption processes," Main Group Chemistry, vol. 21, no. 2, pp. 559-575, Dec. 2021.

[15] J. Su et al., "Hemostatic and antimicrobial properties of chitosan-based wound healing dressings: A review," International Journal of Biological Macromolecules, vol. 306, p. 141570, May 2025.

[16] E. Akdaşçi, H. Duman, F. Eker, M. Bechelany, and S. Karav, "Chitosan and its nanoparticles: A multifaceted approach to antibacterial applications," Nanomaterials, vol. 15, no. 2, p. 126, Jan. 2025.

[17] L. A. Mohammed, O. A. Nief, F. W. Askar, and A. H. Majeed, "Synthesis, characterization and antimicrobial activities of silver nanoparticles coated [1,3] thiazin-4-one derivatives," Journal of Physics: Conference Series, vol. 1294, no. 5, pp. 052028-052028, Sep. 2019.

[18] K. Eickelpasch, P. Lemke, S. Sreekumar, N. Chilukoti, B. M. Moerschbacher, and C. Richter, "A bioactivity matrix for antimicrobial activities of chitosans: A review," International Journal of Biological Macromolecules, vol. 299, p. 140740, Apr. 2025.

[19] P. Kesharwani, Emerging Applications of Carbon Nanotubes in Drug and Gene Delivery. Elsevier, 2022.

[20] S. Nagarajan and K. Arumugam Kuppusamy, "Extracellular synthesis of zinc oxide nanoparticle using seaweeds of Gulf of Mannar, India," Journal of Nanobiotechnology, vol. 11, no. 1, p. 39, 2013.

[21] S. Syed, S. I. Ali, S. R. Ali, and S. K. Sherwani, "Synthesis and characterization of zinc oxide nanoparticles for antibacterial applications," ResearchGate, Apr. 2016.

[22] N. S. Al-Obaidi, Z. S. Al-Garawi, and A. S. Al-Mahdawi, "Polyaniline doping with nanoparticles: A review on the potential of electrical properties," Journal of Physics: Conference Series, vol. 1853, no. 1, pp. 012055-012055, Mar. 2021.

[23] R. F. Melo-Silveira et al., "In vitro antioxidant, anticoagulant and antimicrobial activity and in inhibition of cancer cell proliferation by xylan extracted from corn cobs," vol. 13, no. 1, pp. 409-426, Dec. 2011.

[24] W. F. Wolkers, A. E. Oliver, F. Tablin, and J. H. Crowe, "A Fourier-transform infrared spectroscopy study of sugar glasses," Carbohydrate Research, vol. 339, no. 6, pp. 1077-1085, Apr. 2004.

[25] F. R. F. Silva et al., "Anticoagulant activity, paw edema and pleurisy induced carrageenan: Action of major types of commercial carrageenans," Carbohydrate Polymers, vol. 79, no. 1, pp. 26-33, Jan. 2010.

[26] A. Drabczyk et al., "Physicochemical investigations of chitosan-based hydrogels containing Aloe Vera designed for biomedical use," Materials, vol. 13, no. 14, p. 3073, Jul. 2020.

[27] V. R. Nair, M. Jacob, T. Joseph, and J. T. Varkey, "Applications of chitosan based Schiff bases and its complexes – A review," International Journal of Advanced Research in Science, Communication and Technology, pp. 157-170, Jul. 2021.

[28] A. S. Al-Mahdawi, N. S. Al-Obaidi, A. A. Ahmad, T. A. Jumaa, Z. A. Abas, and H. S. Mahdi, "Synthesis, characterization and evaluation biological activity of some 2-mercaptobinzemidazol complexes," Results in Chemistry, vol. 13, p. 101893, Jan. 2025.

[29] A. Y. Rmaidh, A. S. Al-Mahdawi, N. S. Al-Obaidi, and M. A. Al-Obaidi, "Organic ligands as adsorbent surface of heavy metals and evaluating antibacterial activity of synthesized complexes," Inorganic Chemistry Communications, vol. 156, pp. 111148-111148, Aug. 2023.

[30] M. A. Mohammed, N. S. Al-Obaidi, and S. J. Fadihl, "Investigation of heavy metals and some bacterial species in water stations and evaluate them chemically and biologically in Diyala Governorate, Iraq," Biochemical & Cellular Archives, vol. 18, no. 2, pp. 1921-1925, 2018.